Orientational ordering and correlation in quasi-one-dimensional hard-body fluids due to close-packing degeneracy

Péter Gurin,[1] Sakineh Mizani,[2] and Szabolcs Varga[1]

[1]*Physics Department, Centre for Natural Sciences, University of Pannonia, PO Box 158, Veszprém, H-8201 Hungary*

[2]*Institute for Applied Physics, University of Tübingen, Auf der Morgenstelle 10, 72076 Tübingen, Germany*

(Received 13 April 2024; accepted 20 June 2024; published 15 July 2024)

We study the orientational ordering properties of some quasi-one-dimensional hard-body fluids, where the anisotropic particles are confined to a straight line, while they are free to rotate in a plane. We examine a class of models where the close-packing structure is degenerate, i.e., the highest possible density can be realized with different orientational ordering. We find that the close-packing degeneracy always gives rise to a diverging orientational correlation, which can be a marker of phase transition, glass formation, and jamming. In the case of isotropic or partially ordered phases at the close-packing density, the diverging orientational correlation indicates a tendency for being a strongly ordered nematic phase. However, the orientational divergence in the perfect nematic phase shows that the particles must rotate in concert to go from one closely packed structure to another.

DOI: 10.1103/PhysRevE.110.014702

I. INTRODUCTION

Quasi-one-dimensional (q1D) systems, with their unique interplay between the confinement and particle interactions, have attracted interest in many fields of science [1–8]. A common feature of q1D fluids is that the positional and orientational freedom of the particles is limited to some extent by confining the particles into a very narrow channel [9–15]. These q1D systems exhibit fascinating and often unexpected behaviors, offering a rich playground for studying fundamental phenomena in physics and beyond [16–25]. The research interest ranges from enhancing the alignment of rodlike particles such as gold nanowires and carbon nanotubes with distinctive electrical properties [26–29] to the thermodynamic properties of classical fluids in very narrow pores [30–33]. By exploring the ordering behavior, phase transitions, and collective properties of q1D systems, we can deepen our knowledge to design new nanomaterials with desired physical and chemical properties. By varying the particle shape, particle-particle, and particle-wall interactions, as well as the size of the confining channel, complex structures and phase behaviors can be observed [34–39].

The dimensional restriction can reduce the number of phases and the complexity of the structures, but the phase behavior remains complex. For example, the melting of hard discs in a two-dimensional plane is more complex than that of hard spheres in three dimensions [40]. In one dimension, true phase transitions do not occur in most of the systems [41–45], but they can exhibit anomalous phase behavior [7,46], glass formation [47], and jamming [48]. The advantage of studying q1D systems is that exact results can be obtained in many cases [13,32–34,49,50].

The understanding of the phase behavior of q1D fluids has been the subject of extensive research, leading to several interesting phenomena [51–55]. A remarkable study shows an exceptional example of an infinite number of phase transitions occuring in q1D fluid of soft rods [56]. A first-order phase transition is detected in the system of correlated molecular rotators, which are staying in a q1D array [57]. Notably, the dynamics of a q1D fluid composed of orientable hard rectangles exhibits distinct properties associated with the glass-transition phenomenon, including annealing rate dependence and a characteristic two-step relaxation process [58]. Collectively, these studies provide valuable insights into the complex behavior and the potential for glass formation in q1D systems [59].

In a separate line of inquiry, extensive research has been conducted on the thermodynamic properties of q1D fluids of elongated hard particles [3,4,25,60]. These investigations have uncovered the existence of distinct universality classes based on the geometric attributes of the particles, highlighting the pivotal role of particle morphology in determining orientational fluctuations and correlations. Furthermore, a specific subset of one-dimensional systems, namely a gas composed of needlelike objects, has been thoroughly explored [13,35,61]. These studies significantly contribute to our understanding of the interplay between particle morphology, thermodynamic properties, and orientational behavior in q1D systems [62–66].

The phase behavior of freely rotating hard rods exhibits remarkable similarities to the one-dimensional gas of hard rods studied by Tonks in the limit of close packing [67]. At close packing, the particles lose their ability to rotate, leading us to believe that they become frozen in orientation. However, it was later discovered that even at close packing, orientation fluctuations still contribute to the pressure [34]. Furthermore, Kantor and Kardar found that q1D fluids of hard rods possess other important properties, such as the divergence of the orientational correlation length to infinity at the close-packing density (infinite pressure), specifically observed in systems of hard rectangles but not in systems of ellipses [60]. This suggests that the shape of the constituent particles plays a crucial

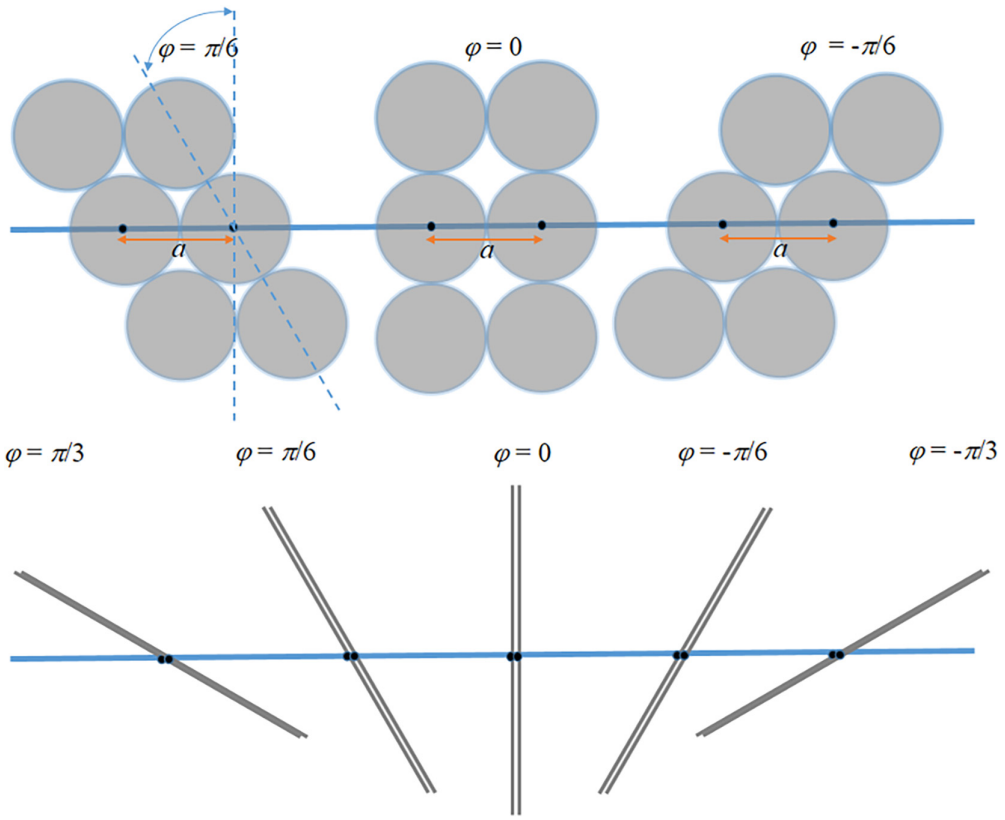

FIG. 1. Quasi-one-dimensional fluid of linear hard chains (upper panel) and that of hard needles (lower panel), which are confined to a straight line, but allowed to rotate freely in a plane. At the close packing the particles must be parallel with each other in both systems. The close packing can be realized with the following angles (φ):$-\pi/6 < \varphi < \pi/6$ for linear chains and $-\pi/2 < \varphi < \pi/2$ for needles.

role in the divergence of the correlation length. Nonetheless, the driving force behind these long-range orientation correlations remains unclear. Therefore, in this study, we aim to investigate the main factor responsible for these long-range orientation correlations by focusing on systems with degenerate close packing.

Our paper is laid out as follows. In Sec. II, we present the distance of closest approach between a pair of particles for three anisotropic hard-body models having degenerate close-packing structures. We show that the system of hard needles and that of linear hard chains, has degenerate close packing if the centers of the particles are confined to a straight line. In Sec. III, we utilize the transfer operator method to investigate the phase behavior and structural properties of three different hard-body systems. In Sec. IV, we present and analyze the results for densities near the close-packing density, which are obtained using both analytical and numerical techniques. Special attention is paid to understand the emergence of diverging orientational correlation length at the close-packing density. Finally, in Sec. V, we present the conclusions of our study and discuss our results in a broader conceptual framework, comparing our results with previous studies.

II. MODELS

We assume that the particles interact with only anisotropic hard repulsive forces and they are restricted in a narrow channel such that the particles form a q1D fluid with only one positional (x) and one orientational (φ) degree of freedom as shown in Fig. 1. We consider such models where the number of close-packing (highest possible density state) configurations is infinite, i.e., the close-packing structure is continuously degenerate in the orientation as it happens in the q1D fluid of linear chains and that of needles in Fig. 1. As the particles must occupy the shortest distance along the channel to get into the close-packing structure, the rodlike particles are parallel, i.e., all particles must have the same orientation at the close packing. This can be achieved with φ angles between $-\pi/6$ and $\pi/6$ for linear chains and with φ angles between $-\pi/2$ and π /2 for needles (see Fig. 1) if φ is restricted to the interval of $-\pi/2 < \varphi < \pi/2$. Note that the up-down symmetry of the rodlike particles does not require to consider other angles in this study. As the particles interact with their first neighbors only, the distance of closest approach between a pair of particles (contact distance for brevity) reflects the close-packing structure of the system. For example, the contact distance of hard needles is given by [61]

$$\sigma(\phi_1, \phi_2) = \frac{l|\sin(\phi_1 - \phi_2)|}{2\max(\cos\phi_1, \cos\phi_2)}, \tag{1}$$

where φ_i is the orientation angle of particle i ($i = 1, 2$) measured from the y axis and l is the length of the needle. This expression shows that the shortest distance between two particles is zero ($\sigma = 0$) if the particles are parallel, i.e., $\varphi_1 = \varphi_2$. Therefore, the close-packing structure of the hard needles is degenerate with respect to the orientation. At this

point it is worth noting that close packing of the fluid of hard ellipses and that of hard rectangles is not degenerate, because all particles have to be aligned with $\varphi = 0$ angles to form close-packing structure. The linear chains can be considered between the needles and the rectangles because $-\pi/6 < \varphi < \pi/6$ is the range of φ degeneracy at the close-packing limit (see Fig. 1).

To understand the role of angle degeneracy of the close-packing structure on the phase behavior and structural properties of q1D fluids, we examine three simple models that have different tendency for orientational ordering. In the first model (M1), the contact distance between two particles is defined by

$$\sigma(\phi_1, \phi_2) = a(1 + [\min(|\phi_1 - \phi_2|, \pi - |\phi_1 - \phi_2|)]^{\alpha}), \quad (2)$$

where "a" is the contact distance between two parallel particles and α is an empirical exponent describing dependence of the contact distance with the change of the angle difference between two particles ($(|\phi_1 - \phi_2|)$).The effect of α is that the cost of orientational fluctuations from the parallel ordering (the increment of σ) is lower with increasing α. In the second model (M2), we assume that

$$\sigma(\phi_1, \phi_2) = a(1 + |\phi_1 - \phi_2|^{\alpha}). \quad (3)$$

In this model $\phi_1 = \phi_2$ produces the shortest distance between two neighboring particles as in M1, but it gives rise to some angle preferences, because the cost of angle fluctuations is lower at angle $\phi = 0$ than at $\phi = \pm\pi/2$, which will be pointed out in the Results, Sec. IV. The third model (M3) is very similar to the hard needles [Eq. (1)] with a slight change that $a = l/2$ and a is added to Eq. (1), i.e.,

$$\sigma(\phi_1, \phi_2) = a\,(1 + \sin|\phi_1 - \phi_2| / \max(\cos\phi_1, \cos\phi_2)) \quad (4)$$

We can see that Eq. (4) is more realistic than Eq. (1) because it gives $\sigma = a$ for $\phi_1 = \phi_2$ orientations instead of $\sigma = 0$, which implies that the system does not become an ideal gas for parallel orientations.

III. TRANSFER OPERATOR METHOD

The phase behavior of a q1D hard-body system with a general contact distance $\sigma(\phi_1, \phi_2)$ can be determined exactly using the well-known transfer operator method [68]. For one-component systems having purely hard-body interactions, the only independent control parameter is βP, where $\beta = 1/(k_B T)$ is the inverse temperature and P is the one-dimensional pressure. The relevant outputs of the transfer operator formalism are the Gibbs free energy (G), the orientational distribution function (f), the orientational order parameter (S), and the orientational correlation function (g_2) in this work. To get these quantities, the following eigenvalue problem has to be solved for λ_i eigenvalue and corresponding ψ_i eigenfunction:

$$\int_{-\pi/2}^{\pi/2} K_i(\phi_1, \phi_2)\,\psi_i(\phi_2)\,d\phi_2 = \lambda_i \psi_i(\phi_1). \quad (5)$$

Here, $K_0(\phi_1, \phi_2) = \exp(-\beta P \sigma(\phi_1, \phi_2))/\beta P$ is the basic kernel for thermodynamic properties, while the higher-order $K_i(\phi_1, \phi_2)$ kernels ($i = 1, 2, \ldots$,etc.) can be obtained by projecting out the lower-order eigenvalues with $K_i(\phi_1, \phi_2) = K_i(\phi_1, \phi_2) - \lambda_{i-1}\psi_{i-1}(\phi_1)\,\psi_{i-1}(\phi_2)$, where the $|\lambda_i| \geqslant |\lambda_{i+1}|$ condition has to be fulfilled. In Eq. (5) it is assumed that the eigenfunctions are normalized as follows: $\int_{-\pi/2}^{\pi/2} \psi_i^2(\phi)\,d\phi = 1$. Under the above circumstances, we get the Gibbs free-energy density ($g = \beta G/N$), the one-dimensional number density ($\rho = N/L$), f and S using the largest eigenvalue (λ_0), and the corresponding eigenfunction (ψ_0) as follows: $g = -\ln\lambda_0$, $\rho^{-1} = \frac{dg}{d(\beta P)}$, $f(\phi) = \psi_0^2(\phi)$, and $S = \int_{-\pi/2}^{\pi/2} \cos(2\phi) f(\phi) d\phi$, where N is the number of particles and L is the length of the channel. We also determine angle fluctuation from the orientational distribution function as follows: $\langle\phi^2\rangle = \int_{-\pi/2}^{\pi/2} \phi^2 f(\phi) d\phi$, because $\langle\phi\rangle = \int_{-\pi/2}^{\pi/2} \phi f(\phi) d\phi = 0$.

The orientational correlation function, which is defined as $g_2(i) = \langle\cos(2\phi(0) - 2\phi(i))\rangle - S^2$ [13,68], can be obtained with the help of higher-order eigenvalues and the corresponding eigenfunctions using

$$g_2(i) = \sum_{j=1}^{\infty} \left(\frac{\lambda_j}{\lambda_0}\right)^i \left(\left[\int_{-\pi/2}^{\pi/2} \cos(2\phi)\,\psi_0(\phi)\,\psi_j(\phi) d\phi \right]^2 + \left[\int_{-\pi/2}^{\pi/2} \sin(2\phi)\,\psi_0(\phi)\,\psi_j(\phi) d\phi \right]^2 \right), \quad (6)$$

where i denotes the ith neighbor from a given particle, i.e., there are $i - 1$ particles between a particle j and a particle $j + i$. We can see from Eq. (6) that g_2 decays exponentially as i goes to ∞, i.e., $g_2(i \to \infty) \approx \exp(-i/\xi)$, where ξ is the orientational correlation length. As $\lambda_0 > \lambda_1 > \lambda_2 > \ldots$, the leading term of Eq. (6) is $(\lambda_1/\lambda_0)^i$, and we can get from $\exp(-i/\xi) = (\lambda_1/\lambda_0)^i$ that

$$\xi^{-1} = \ln\left(\frac{\lambda_0}{\lambda_1}\right) \quad (7)$$

This shows that the orientational correlation is very weak if $\lambda_0 >> \lambda_1$, while it diverges if λ_0/λ_1 goes to 1. It is very easy to prove that there is no orientational correlation if the contact distance is constant, which corresponds to the system of hard spheres confined to a straight line. In this system, the contact distance is identical with the diameter of the sphere (a), i.e., $\sigma = a$. It is trivial to show that $\lambda_0 = \pi\exp(-\beta P a)/\beta P$ and $\psi_0 = 1/\sqrt{\pi}$ are the solutions of Eq. (5) for $i = 0$. Using these results we get that $K_i(\phi_1, \phi_2) = 0$ for $i > 0$, which implies that all higher-order eigenvalues are zero ($\lambda_i = 0$, where $i = 1, 2, \ldots$,etc.). As λ_0/λ_1 is infinite for hard spheres, Eq. (7) shows the trivial result that the orientational correlation length is always zero. The other trivial result is that the phase is always isotropic as $f = 1/\pi$ and $S = 0$. Moreover, we can derive the well-known Tonks equation of state of hard rods [67] using $g = \frac{\beta G}{N} = -\ln\lambda_0$ and $\rho^{-1} = \frac{dg}{d(\beta P)}$, which is given by

$$\beta P_T = \frac{\rho}{1 - \rho a}. \quad (8)$$

However, the solution of the eigenvalue problem [Eq. (5)] is not trivial for the orientation-dependent contact distances. We present our analytical results for M1 system, which is defined by Eq. (2). Moreover, numerical calculations are performed for M2 and M3 systems, which are defined with contact distances given by Eqs. (3) and (4), respectively. To

get reliable numerical results, we used very fine grid sizes to perform the integration with respect to the orientation (φ), because the orientational ordering can be very strong in the vicinity of close packing. It turned out that an equidistance representation of the orientation with $d\varphi = \pi/5000$ grid size, i.e., $\varphi_i = -\pi/2 + id\varphi$, is satisfactory to get the accurate results for the eigenvalues and eigenfunctions using the successive iteration method. Our initial guess for the eigenfunction ($\psi_i(\phi)$) was $1/\sqrt{\pi}$ for all systems. We found that the convergence of the iteration is very fast with this guess, and the maximum iteration number does not exceed 5000 steps. Finally, we mention that the results are presented in dimensionless units using a and β, i.e., $\rho^* = \rho a$ is the dimensionless density and $\rho^* = \beta P a$ is the dimensionless pressure.

IV. RESULTS

The phase behavior and the structural properties of the system M1 can be obtained analytically. The exact solution relies on the fact that the contact distance defined by Eq. (2) can be extended for any values of $-\infty < \varphi_1, \varphi_2 < \infty$ fulfilling the following two requirements at the same time: (i) $\sigma(\varphi_1, \varphi_2)$ is a periodic function in both variables with π, and (ii) σ depends only on $|\varphi_1 - \varphi_2|$. We must mention here that these two requirements are not fulfilled by M2 given by Eq. (3). Without going into the details, we present the results of the eigenvalue problem [Eq. (5)] for the contact distance given by Eq. (2). It can be shown that the eigenvalues are given by

$$\lambda_i = \frac{\exp(-\beta P a)}{\beta P} \int_{-\pi/2}^{\pi/2} \cos(2i\phi) \exp(-\beta P |\phi|^\alpha)\, d\phi, \quad (9)$$

where $i = 0, 1, 2, \ldots$,etc. The highest eigenvalue is λ_0, while the corresponding eigenfunction is given by $\psi_0(\phi) = 1/\sqrt{\pi}$. This means that the phase is isotropic for all possible values of the pressure, because the orientational distribution is constant as $f = \psi_0^2 = 1/\pi$. The higher-order eigenvalues (λ_i, where $i = 1, 2, \ldots$,etc.) are twofold degenerate with $\psi_{i,1}(\phi) = \sqrt{\frac{2}{\pi}} \cos(2i\phi)$ and $\psi_{i,2}(\phi) = \sqrt{\frac{2}{\pi}} \sin(2i\phi)$ eigenfunctions (see the Supplemental Material for further details [69]). From λ_0 we can get the thermodynamic properties of the system, while the higher-order eigenvalues and the corresponding eigenfunctions provide information about the orientational ordering. Now we focus on the high-pressure limit, which pushes the system into the close-packing structure. Let us introduce a variable z from φ as follows $z := (\beta P)^{1/\alpha}\phi$. As the exponential function in Eq. (9) goes to zero very fast with increasing pressure, we can change the integration boundaries from finite range to infinite, i.e., $\int_{-\pi/2}^{\pi/2} \ldots d\phi \Leftrightarrow \frac{1}{(\beta P)^{1/\alpha}} \int_{-\infty}^{\infty} \ldots dz$. Furthermore we can use the following second-order Taylor-expansion: $\cos(2i\phi) \approx 1 - 2i^2\phi^2$. Using the introduced variable (z) and the above approximations, we get from Eq. (9) that

$$\lambda_i = \lambda_0 - \frac{\exp(-\beta P a)}{(\beta P)^{1+1/\alpha}} \frac{2i^2}{(\beta P)^{2/\alpha}} \int_{-\infty}^{\infty} z^2 \exp(-|z|^\alpha) dz, \quad (10)$$

where $\lambda_0 = \frac{\exp(-\beta P a)}{(\beta P)^{1+1/\alpha}} \int_{-\infty}^{\infty} \exp(-|z|^\alpha)\, dz$ is the largest eigenvalue. As $g = -\ln \lambda_0$ and $\rho^{-1} = dg/d(\beta P)$, we get the equation of state of the M1 in the high-pressure limit as follows:

$\beta P = (1 + 1/\alpha)\frac{\rho}{1-\rho a}$. Therefore, the deviation of the pressure of the M1 system and that of Tonks-gas [see Eq. (8)] can be written as

$$P/P_T = 1 + 1/\alpha. \quad (11)$$

We can see from this equation that only the α parameter affects the deviation from the Tonks gas at high pressures. As the deviation is due to the orientational freedom of the model, the orientational fluctuation has a P_T/α contribution to the pressure of the orientationally frozen Tonks equation of state. Since the increment in the contact distance due to the orientational fluctuations ($\Delta\phi$) is proportional to $|\Delta\phi|^\alpha$, the deviation from the Tonks gas becomes stronger with decreasing α, because the contact distance increases more for lower α values at a given $\Delta\phi$ fluctuation. In the same manner we can calculate the correlation length from Eq. (7) in the high-pressure limit. Using Eq. (10) we can write that

$$\lambda_i/\lambda_0 \approx \left\{ 1 - \frac{2i^2}{(\beta P)^{2/\alpha}} \frac{\int_{-\infty}^{\infty} z^2 \exp(-|z|^\alpha) dz}{\int_{-\infty}^{\infty} \exp(-|z|^\alpha) dz} \right\}. \quad (12)$$

After substitution of this equation into Eq. (7) we end up with

$$\xi^{-1} \approx \frac{2}{(\beta P)^{2/\alpha}} \frac{\int_{-\infty}^{\infty} z^2 \exp(-|z|^\alpha) dz}{\int_{-\infty}^{\infty} \exp(-|z|^\alpha) dz}, \quad (13)$$

where the integrals do not depend on the pressure. Therefore, the correlation length in model M1 at very high pressures is given by

$$\xi \sim (\beta P)^{2/\alpha}. \quad (14)$$

This shows that the M1 model is an orientationally strongly correlated system and the correlation length diverges with the pressure. This system becomes uncorrelated at high pressures only if $\alpha \to \infty$, where the cost of fluctuation goes to zero in the contact distance.

The results from Eq. (9) for both low and high pressures are shown in Fig. 2. We can see the effect of α on the equation of state in Fig. 2(a). When comparing the pressures at a given value of density (ρ^*), it is observed that the pressure is consistently higher for $\alpha = 1$, compared to $\alpha = 2$. This difference in pressure can be attributed to the disparity in the cost of fluctuations between the two cases. Specifically, the cost of fluctuations in the contact distance is greater for $\alpha = 1$ than for $\alpha = 2$. The inset of Fig. 2(a) illustrates the deviation from the Tonks equation of state. Notably, the deviation from the Tonks gas behavior is more pronounced for $\alpha = 1$, with P/P_t precisely converging to 2, whereas it converges to 1.5 for $\alpha = 2$. This is due to the fact that M1 with $\alpha = 1$ has a larger collision diameter compared to the case of $\alpha = 2$. Therefore, the increased collision diameter implies the higher pressure. Note that these results are consistent with our high-pressure result [see Eq. (11)]. Figure 2(b) shows orientational correlation length as a function of pressure for $\alpha = 1$ and 2. It is evident that the system with $\alpha = 1$ exhibits stronger correlations due to the higher cost of fluctuations compared to the case of $\alpha = 2$. The results show that there

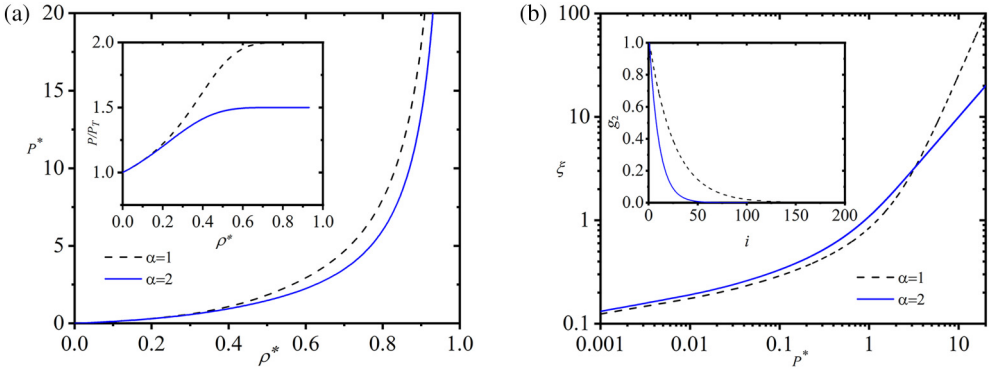

FIG. 2. The effect of α on the equation of state (a) and the orientational correlation length (b) of Model 1 (M1), which is defined by Eq. (2). The inset of (a) highlights the deviation from the Tonks equation of state, while the orientational correlation function between two particles is presented at $P^* = 10$ in the inset of (b). The pressure and the density are dimensionless, i.e., $P^* = \beta P a$ and $\rho^* = \rho a$. The parameter i counts the number of particles between two chosen particles.

is a crossover point in the pressure, below which $\alpha = 2$ displays a higher correlation, while above this point the trend reverses, indicating that the system with $\alpha = 1$ becomes more correlated. Furthermore, the curves are linear in log-log scale at higher pressures, indicating that Eq. (14) becomes valid for pressures above the crossover point. Remarkably, the slopes of the curves are consistent with the prediction of Eq. (14). The inset of Fig. 2(b) presents the results of Eq. (6) using 20 eigenvalues and the corresponding eigenfunctions of the M1 system at $P^* = 10$. It can be seen that for $\alpha = 1$, the system exhibits stronger correlations, as the correlation function reaches zero at higher distances compared to the case of $\alpha = 2$. The stronger orientational correlation of $\alpha = 1$ case is due to the higher contact distance cost coming from the orientational fluctuations.

We now proceed to present the results of Model 2 (M2), which is defined by the contact distance given by Eq. (3). Our results are presented for the equation of state, orientational correlation length, and the order parameter in Fig. 3. As for the M1 system, it can be seen that for $\alpha = 1$, the pressure consistently surpasses that of $\alpha = 2$. This deviation in pressure can be attributed to the differences in the cost of fluctuations between the two cases, similar to the observations in the M1 model. However, the deviation from the Tonks equation of state does not follow the M1 system, because the curves of $\alpha = 1$ and those of $\alpha = 2$ cases cross each other at an intermediate density [see the inset of Fig. 3(a)]. As we learned in the M1 system, if the fluctuations are costly in terms of contact distance, the pressure deviates significantly from the Tonks gas behavior. Therefore, we can say that the emergence of a density cross point suggests that the fluctuation cost is higher in the contact distance for $\alpha = 2$ than for $\alpha = 1$ at low densities, while the opposite trend happens at high densities. We can also see in the inset of Fig. 3(a) that the high-pressure behavior of the M2 system is the same as that of the M1 system, since Eq. (11) is also valid for the M2 system. This unexpected results is obtained in light of the fact that fluctuation cost in the contact distance is higher in the M2 system, because the "*min*" function is missing in the definition of the M2 system [compare Eqs. (2) and (3)]. This particular characteristic is due to the fact that when the angle between two particles exceeds $\pi/2$, the contact distance is even larger than in the M1 case. Figure 3(b) reveals a negligible difference in the orientational correlation between M1 and M2 systems, as the contact distance remains nearly identical in both cases when the neighboring particles are almost parallel to each other at high pressures. An additional figure [Fig. 3(c)] is included to compare the M2 with the M1, as the M2 tends to exhibit some level of ordering, albeit not strongly pronounced. The system displays orientational ordering, as evidenced by the nonzero order parameter. Interestingly, the M2 system is only partially ordered, with the orientational order parameter not converging to 1 at high densities, which would be the typical value of the order parameter at the close-packing density. It can be proved exactly for $\alpha = 1$ that $\psi_0(\phi) = \sqrt{\frac{2}{\pi}}\cos(\phi)$ in the limit of $P \to \infty$ [70]. Using this expression one can get that $S = \langle \cos(2\phi) \rangle = 1/2$ and $\langle \varphi^2 \rangle = \pi^2/12 - 1/2 \approx 0.32$. It is worth noting here that $\langle \varphi^2 \rangle = \pi^2/12 \approx 0.82$ in the M1 system, which is isotropic at all possible densities. In the case of $\alpha = 2$, we could get the limiting values $S \approx 0.485$ and $\langle \phi^2 \rangle \approx 0.34$ with only numerical solution of the eigenvalue problem. We can see that the M2 system with $\alpha = 1$ is more ordered with lower one-particle average fluctuation than that of the M2 with $\alpha = 2$. These results are the consequence of the cost of orientational fluctuation on the contact distance. However, it is not trivial to understand why the M2 system exhibits orientational ordering with a peak at $\varphi = 0$ as the close packing of the system is degenerated in the angle φ. The answer for this issue is that cost of orientational fluctuation is the lowest around $\varphi = 0$, while it is highest around $\varphi = \pm\pi/2$ in the contact distance. Therefore, we can say the fluctuation-induced orientational ordering occurs in the M2 system, which results in a nematic ordering with a director at $\varphi = 0$.

Finally, in Fig. 4 we present our numerical results for the M3 system, which is more strongly ordered than the previous systems. The equation of state seems to be very similar to the M1 and M2 system, because P/P_T converges to 2 at the close-packing density, which corresponds to the $\alpha = 1$ case in the previous systems. However, P/P_T is a nonmonotonic function of ρ as it has an intermediate peak at around $\rho^* = 0.5$ with a value of $P/P_T \approx 2$ [see Fig. 4(a)]. The slope of the

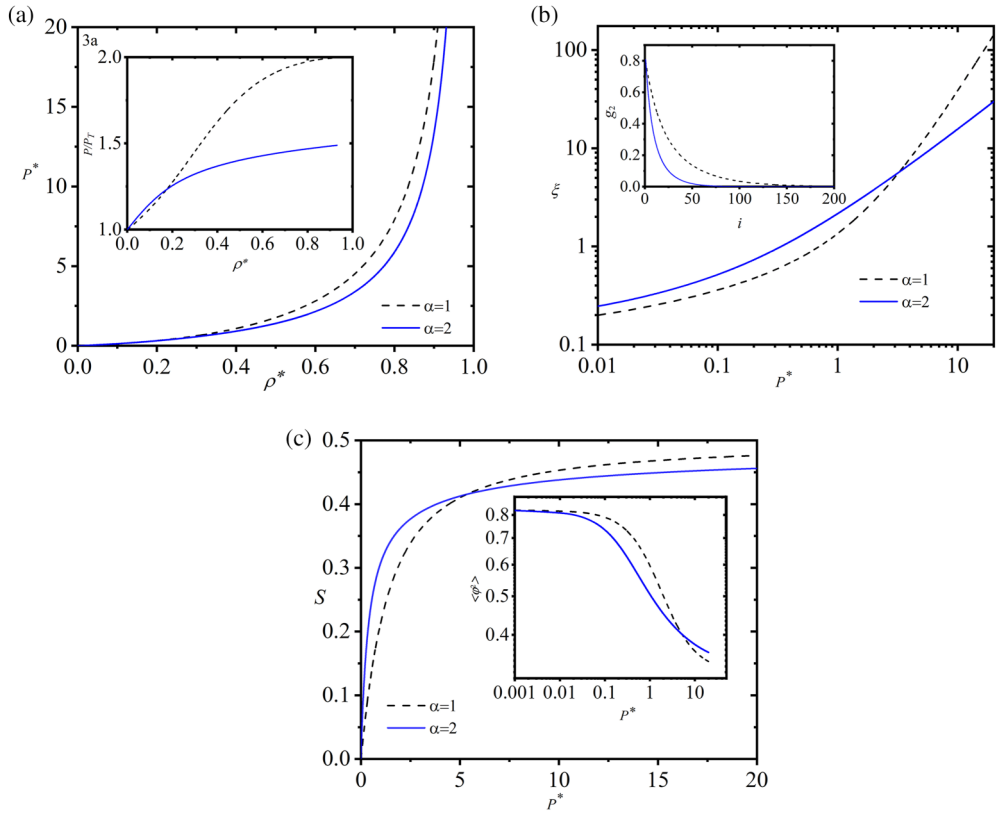

FIG. 3. The effect of α on the equation of state (a), the orientational correlation length (b) and the orientational order parameter (c) of Model 2 (M2), which is defined by Eq. (3). The insets show the deviation from the Tonks equation of state in (a), the orientational correlation function between two particles at $P^* = 10$ in (b), and the average angle fluctuation in (c). The pressure and the density are dimensionless, i.e., $P^* = \beta P a$ and $\rho^* = \rho a$. The parameter i counts the number of particles between two chosen particles.

correlation length is also nonmonotonic in log-log scale, showing that the pressure dependence of the correlation is different at intermediate and high pressures [see Fig. 4(b)]. The order parameter goes to the limiting $S = 1$ with increasing pressure, but the angle fluctuation decreases slowly up to $P^* = 1$, then algebraically decays to zero with increasing pressure [see Fig. 4(c)]. These results show together that the phase behavior of the M3 model is very similar to that of the M2 up to intermediate pressures, because P/P_T tries to saturate at 2 and $\langle\varphi^2\rangle$ decreases slowly as it happens in the M2 system. As $P/P_T \approx 2$, α equals to 1 in the corresponding M2 system. However, the M3 system behaves very differently at very high pressures, as the orientational correlation becomes weaker ($\xi \sim P$) and the orientational fluctuation vanishes according to $\langle\varphi^2\rangle \sim 1/P$. These results do not follow $\xi \sim P^{2/\alpha}$ law [see Eq. (14)] and $\langle\varphi^2\rangle$ is not finite at infinite pressure, which are valid for both M1 and M2 models. Interestingly, $P/P_T = 1 + 1/\alpha$ holds for all models, if α is taken to be 1.

These results show that the M3 system can be considered as another class of q1D fluids, because it behaves differently from M1 and M2 systems and it does not belong to the previously studied q1D hard-body systems, where either no diverging orientational correlation is observed [34] or the divergence goes with $P^{1/2}$ [60]. Regarding the meaning of the diverging orientatinal correlation, it cannot be the indicator of an orientational phase transition, because the system is perfectly ordered at the close-packing density. It is more likely that the diverging correlation length is the marker of the jamming proposed by Kantor and Kardar [60], because each particle is stuck between neighboring particles suppressing their rotational fluctuations. Although, the transition between different close-packing states can be made by *global* rotation, and these states are not separated by energy barriers as in the case of the ordinary glassy systems, these different close-packing states are far from each other in the sense that *random* fluctuations cannot drive the system from one closely packed state to another. Therefore, the diverging correlation length indicates that the only way to go from one closely packed structures with a given tilt angle to the other one with a different tilt angle is to do it in concert, i.e., all particles must do the same rotation in the same time, while random thermal fluctuations cannot change this jammed state of the system.

In summary, due to the effect described in the previous paragraph, the correlation length diverges with the increasing pressure in all three models studied. The key to a deeper understanding of this result is that a single close-packing state is associated with the same orientation of all particles. Nevertheless, the orientational ordering is different, because there are many close-packing states, so the average of these states and fluctuations around them can lead to isotropic ordering (M1), or partial ordering (M2), or complete ordering (M3). The difference among them is due to the fluctuations around the close-packing states. In the case of model M1, the neighborhoods of all close-packing states are completely

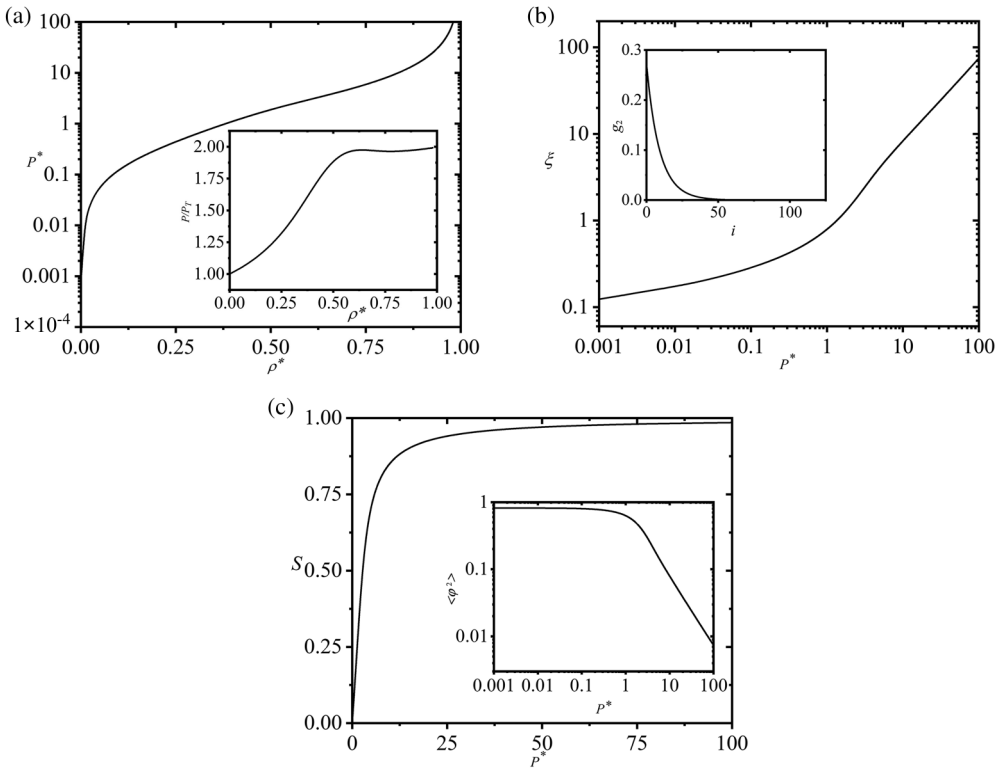

FIG. 4. The effect of α on the equation of state (a), the orientational correlation length (b), and the orientational order parameter (c) of Model 3 (M3), which is defined by Eq. (4). The insets shows the deviation from the Tonks equation of state in (a), the orientational correlation function between two particles at $P^* = 10$ in (b), and the average angle fluctuation in (c). The pressure and the density are dimensionless, i.e., $P^* = \beta Pa$ and $\rho^* = \rho a$. The parameter i counts the number of particles between chosen two particles.

equivalent, the fluctuations behave in the same way around every close-packing state, giving rise to an isotropic order ($S = 0$). In the case of model M3, the small fluctuations in the angle of a given particle has less cost (the increment in the contact distance is smaller) in the case when the orientation of the neighboring particles are perpendicular to the confining line. As the neighboring particles tilt out from the perpendicular direction, the cost of the fluctuation increases. Therefore, the system prefers the perpendicular orientation in spite of the fact that the close-packing degeneracy is the same as in the case of model M1. As a result, the angular fluctuations stabilize the nematic order along the perpendicular direction. The second model (M2) is between M1 and M3. The cost of small fluctuations in the relative angle is the same at almost every angle except the cases when the particles are parallel with the confining line, i.e., $\varphi_1 = \pm\pi/2$ and $\varphi_2 = \pm\pi/2$. In these special situations an infinitesimal fluctuation increases the contact distance with a finite value, because the contact distance is not a continuous function. Therefore, these particular points are very unfavorable and behave like walls, i.e., the parallel particles cannot rotate freely together either. Therefore, although at high pressure the relative fluctuations of neighboring particles behave in the same way for almost all orientations, the collective fluctuations will still prefer the perpendicular orientation, because they can be the largest in these orientations. However, these effects cannot completely order the system, so the order parameter does not reach 1 even at infinite pressure.

V. CONCLUSIONS

In this study, an in-depth investigation has been conducted to understand the orientational ordering properties of three different q1D hard-body fluids having degenerate structures at the close-packing density. We have unraveled important insights into the phase behavior, structural characteristics, and collective features of these systems. We have paid special attention to the pressure, orientational correlation, and angular fluctuation in the vicinity of close-packing density, which can be realized with very high pressures along the channel. It has been observed that the fluids of three models can be described with the same equation of state at high pressures as $P/P_T = 1 + 1/\alpha$ holds for all of them. However, this agreement does not imply that the order parameter, the angular fluctuation, and the orientation correlation have the same properties in the three systems studied. For example, the orientational ordering properties are very different in each system, because M1 shows no orientational ordering at all, M2 shows partial ordering, and M3 is perfectly ordered at the close-packing density. The orientational correlation length diverges with pressure ($\xi \sim P^{2/\alpha}$) in M1 and M2 systems, while the correlation weakens in the third model as $\xi \sim P$. The angular fluctuation is also different in these models: $\langle\varphi^2\rangle = \pi^2/12 \approx 0.82$ for M1, $\langle\varphi^2\rangle = \pi^2/12 - 1/2 \approx 0.32$ for M2, and $\langle\varphi^2\rangle \sim 1/P$ for M3 at the close-packing density. From these results we can conclude that only the M1system shows critical behavior at the close-packing density ($\rho^* = 1$), be-

cause it is in isotropic phase in the whole range of density and the orientational correlation length diverges to infinity at $\rho^* = 1$. Therefore, the system would undergo a spontaneous symmetry-breaking phase transition from the isotropic ($S = 0$) to the perfectly ordered nematic phase ($S = 1$), and $\xi \to \infty$ indicates that a system would choose a director randomly, which will be the orientation of all particles at $\rho^* = 1$. In the case of the M2 system, there is no possibility for symmetry-breaking transition, because the system is already partially ordered with a peak in the orientational distribution function at $\varphi = 0$. Therefore, the diverging ξ marks that the system would jump from a partially ordered phase to a perfectly ordered one. Finally, the M3 system does not show any tendency for critical behavior, because it is perfectly ordered at $\rho^* = 1$. In this system, the diverging correlation length and the vanishing orientational fluctuation are the signals of the entropy cost from moving from one degenerate close-packing structure to the other one. This is the only way to alter the director of the fully correlated M3 system if all particles change their orientations with the same angle at the same time.

To understand better the phase behavior of the M3 system, we review the earlier q1D models, which are devised for ellipse, rectangle, and other shapes to determine the phase behavior of nonspherical hard-body fluids at high pressure. The contact distance of the first class is due to Lebowitz *et al.* [34], which can be written as

$$\sigma(\phi_1, \phi_2) = a + b|\phi_1 + \phi_2|^\alpha + c\,|\phi_1 - \phi_2|^\alpha, \tag{15}$$

where a, b, and c are shape-dependent parameters. The second class of models belongs to Kantor and Kardar [60], which is given by

$$\sigma(\phi_1, \phi_2) = a + b\left(\phi_1^2 + \phi_2^2\right) + c|\phi_1 - \phi_2|^\alpha. \tag{16}$$

The third class can be obtained with the Taylor expansion of Eq. (4) around $\varphi_1 = \varphi_2 = 0$. It can be shown that

$$\sigma(\phi_1, \phi_2) = a + b|\phi_1 - \phi_2|^\alpha + c|\phi_1 - \phi_2|^\alpha \min\left(\phi_1^2, \phi_2^2\right), \tag{17}$$

where a is the contact distance for parallel orientations, $b = a$, $c = a/2$, and $\alpha = 1$ for the contact distance given by Eq. (4). Note that Eq. (17) can be also used for hard needles with length l, with $a = 0$, $b = l/2$, $c = l/4$, and $\alpha = 1$. We have checked the results coming from Eq. (17) are really identical with that of Eq. (4) at high pressures. We summarize our results of the transfer operator calculations using the above three classes of contact distances in Table I. We can see that all classes of models can be described with the same equation of state, i.e., $\beta P = (1 + 1/\alpha)\,\beta P_T$ provides the pressure in the vicinity of the close-packing densities, where $\beta P_T = \rho/(1 - \rho a)$. However, the pressure dependence of the orientational correlation is very different in these classes of models: (i) the first class is uncorrelated for any value of α; (ii) the second class is uncorrelated for $\alpha = 2$ and weakly correlated for $\alpha = 1$; and (iii) the third class is correlated even for $\alpha = 2$. The angular fluctuations has a $\langle\varphi^2\rangle \sim P^{-2/\alpha}$ dependence in the first class; it vanishes very similarly in the second class and it has a weaker dependence from the pressure in the third class of model. A common feature of all classes is that the angular fluctuation weakens with decreasing α, while the orientational correlation becomes stronger in the second and third classes. It can also be concluded that the models belonging to second class are always more ordered that those of the third one is due to the second term in Eq. (16), which forces the particles to be parallel with $\varphi = 0$ angles, while the second term of Eq. (17) gives rise to a weak orientational order as it happens in the M2 system. This is also why the third class shows a higher correlation than the second class for the same α value. In the third class, the third term of Eq. (17) is responsible for the perfect orientational order at the close-packing density, because the second one causes only a partial orientational order. However, it can be also seen that the third term is a lower-order term than the second term. The consequence of this fact is that the ordering properties of systems belonging to third class is determined mainly by the second term at the low- and intermediate densities, while the third term becomes relevant in the vicinity of close-packing density. This fact manifests in the ordering properties of the M3 system, which behaves very similarly to the M2 system at intermediate densities, but shows very different behavior at the close packing. This can be seen as an intermediate peak in the P/P_T vs ρ^* curve and an inflection point arises in ξ vs P curve.

TABLE I. High-pressure behavior of three classes of models, which are defined by Eqs. (15)–(17).

	Eq. (15)	Eq. (15)	Eq. (16)	Eq. (16)	Eq. (17)	Eq. (17)
	$\alpha = 1$	$\alpha = 2$	$\alpha = 1$	$\alpha = 2$	$\alpha = 1$	$\alpha = 2$
P/P_T	2	1.5	2	1.5	2	1.5
ξ	P^0	P^0	$P^{0.5}$	P^0	P^1	$P^{0.47}$
$\langle\varphi^2\rangle$	P^{-2}	P^{-1}	$P^{-1.5}$	P^{-1}	P^{-1}	$P^{-0.53}$

To describe the high-pressure behavior of anisotropic hard-body fluids, the important contribution of the contact distance depends on the shape of the particles. For hard needles, the third class is the right model, while the second one can be used for rectangles. However, it is not clear what the minimum model is for other particles' shape, such as rigid and flexible hard chains. It is also an issue how these fluids behave and correlate at the close-packing density. We leave these issues for future studies.

ACKNOWLEDGMENTS

P.G. and S.V. gratefully acknowledge the financial support of the National Research, Development, and Innovation Office, Grants No. NKFIH K137720 and No. TKP2021-NKTA-21. S.M. expresses her appreciation for insightful discussions with Martin Oettel.

[1] B. C. Freasier and L. K. Runnels, J. Chem. Phys. **58**, 2963 (1973).

[2] S. Romano, Il Nuovo Cim. D **10**, 1459 (1988).

[3] C. F. Tejero and J. A. Cuesta, Physica A Stat. Mech. Appl. **168**, 942 (1990).
[4] B. Martínez-Haya, J. M. Pastor, and J. A. Cuesta, Phys. Rev. E **59**, 1957 (1999).
[5] T. Giamarchi, Chem. Rev. **104**, 5037 (2004).
[6] M. Moradi and F. Taghizadeh, Physica A Stat. Mech. Appl. **387**, 6463 (2008).
[7] P. Gurin and S. Varga, Phys. Rev. E **106**, 044606 (2022).
[8] M. Wilkinson, arXiv:2311.00446 (2023).
[9] H. Moraal, Physica A: Stat. Mech. Appl. **85**, 457 (1976).
[10] J. L. Lebowitz and J. K. Percus, Ann. N. Y. Acad. Sci. **410**, 351 (1983).
[11] J. Szulga, W. A. Woyczynski, B. Ycart, and J. A. Mann, J. Stat. Phys. **46**, 67 (1987).
[12] S. Y. Zhang, M. D. Regulacio, and M. Y. Han, Chem. Soc. Rev. **43**, 2301 (2014).
[13] P. Gurin and S. Varga, Phys. Rev. E **83**, 061710 (2011).
[14] A. N. Generalova, V. A. Oleinikov, and E. V. Khaydukov, J. Colloid Interface Sci. **297**, 102543 (2021).
[15] V. M. Pergamenshchik, T. Bryk, and A. Trokhymchuk, J. Mol. Liq. **387**, 122572 (2023).
[16] M. E. Fisher and B. Widom, J. Chem. Phys. **50**, 3756 (1969).
[17] J. M. Brader and R. Evans, Physica A: Stat. Mech. Appl. **306**, 287 (2002).
[18] S. Liu, J. B. H. Tok, J. Locklin, and Z. Bao, Small **2**, 1448 (2006).
[19] Q. Zhang, S. Gupta, T. Emrick, and T. P. Russell, J. Am. Chem. Soc. **128**, 3898 (2006).
[20] Q. Y. Tang and Y. Q. Ma, J. Phys. Chem. B **113**, 10117 (2009).
[21] B. Lin, D. Valley, M. Meron, B. Cui, H. M. Ho, and S. A. Rice, J. Phys. Chem. B **113**, 13742 (2009).
[22] M. Moradi and S. Hashemi, Eur. Phys. J. B **84**, 289 (2011).
[23] W. Li, P. Zhang, M. Dai, J. He, T. Babu, Y. L. Xu, R. Deng, R. Liang, M. H. Lu, Z. Nie, and J. Zhu, Macromolecules **46**, 2241 (2013).
[24] L. Aramis, S. A. Kraemer, G. Odriozola, and M. López de Haro, Mol. Phys. e2307499 (2024).
[25] D. B. Liarte, A. Petri, and S. R. Salinas, Braz. J. Phys. **53**, 73 (2023).
[26] X. He, W. Gao, L. Xie, B. Li, Q. Zhang, S. Lei, J. M. Robinson, E. H. Hároz, S. K. Doorn, W. Wang, and R. Vajtai, Nat. Nanotechnol. **11**, 633 (2016).
[27] O. Jahanmahin, D. J. Kirby, B. D. Smith, C. A. Albright, Z. A. Gobert, C. D. Keating, and K. A. Fichthorn, J. Phys. Chem. C **124**, 9559 (2020).
[28] K. R. Jinkins, S. M. Foradori, V. Saraswat, R. M. Jacobberger, J. H. Dwyer, P. Gopalan, A. Berson, and M. S. Arnold, Sci. Adv. **7**, eabh0640 (2021).
[29] S. Mizani, S. Naghavi, and S. Varga, J. Mol. Liq. **392**, 123432 (2023).
[30] J. F. Marko, Phys. Rev. Lett. **62**, 543 (1989).
[31] V. M. Pergamenshchik, J. Chem. Phys. **153**, 144111 (2020).
[32] A. M. Montero and A. Santos, J. Chem. Phys. **158**, 154501 (2023).
[33] A. M. Montero and A. Santos, J. Chem. Phys. **159**, 034503 (2023).
[34] J. L. Lebowitz, J. K. Percus, and J. Talbot, J. Stat. Phys. **49**, 1221 (1987).
[35] P. Gurin and S. Varga, Phys. Rev. E **82**, 041713 (2010).
[36] A. Mughal, H. K. Chan, and D. Weaire, Phys. Rev. Lett. **106**, 115704 (2011).
[37] M. Z. Yamchi and R. K. Bowles, Phys. Rev. Lett. **115**, 025702 (2015).
[38] W. Jin, H. K. Chan, and Z. Zhong, Phys. Rev. Lett. **124**, 248002 (2020).
[39] E. Basurto, P. Gurin, S. Varga, and G. Odriozola, J. Mol. Liq. **333**, 115896 (2021).
[40] P. Gurin, S. Varga, and G. Odriozola, Phys. Rev. E **102**, 062603 (2020).
[41] T. T. M. Vo, L. J. Chen, and M. Robert, J. Chem. Phys. **119**, 5607 (2003).
[42] C. Grodon, M. Dijkstra, R. Evans, and R. Roth, Mol. Phys. **103**, 3009 (2005).
[43] Y. Liu, Q. Wang, L. Zhang, and T. Wu, Langmuir **21**, 12025 (2005).
[44] B. P. Khanal and E. R. Zubarev, Angew. Chem. **119**, 2245 (2007).
[45] M. Schwartz, Physica A: Stat. Mech. Appl. **389**, 731 (2010).
[46] Y. Hu and P. Charbonneau, Phys. Rev. Res. **3**, 038001 (2021).
[47] Y. Zhang, M. J. Godfrey, and M. A. Moore, Phys. Rev. E **102**, 042614 (2020).
[48] S. S. Ashwin and R. K. Bowles, Phys. Rev. Lett. **102**, 235701 (2009).
[49] M. A. G. Maestre and A. Santos, J. Stat. Mech.: Theory Exp. (2020) 063217.
[50] P. J. Reynolds, H. E. Stanley, and W. Klein, J. Phys. A: Math. Gen. **10**, L203 (1977).
[51] E. Kierlik and M. L. Rosinberg, J. Stat. Phys. **68**, 1037 (1992).
[52] E. Trizac and I. Pagonabarraga, Am. J. Phys. **76**, 777 (2008).
[53] J. Köfinger and C. Dellago, N. J. Phys. **12**, 093044 (2010).
[54] B. D. Marshall, Phys. Rev. E **94**, 012615 (2016).
[55] A. M. Montero and A. Santos, arXiv:2405.03362 (2024).
[56] S. Saryal, J. U. Klamser, T. Sadhu, and D. Dhar, Phys. Rev. Lett. **121**, 240601 (2018).
[57] L. M. Casey and L. K. Runnels, J. Chem. Phys. **51**, 5070 (1969).
[58] J. J. Arenzon, D. Dhar, and R. Dickman, Phys. Rev. E **84**, 011505 (2011).
[59] R. K. Bowles, Physica A: Stat. Mech. Appl. **275**, 217 (2000).
[60] Y. Kantor and M. Kardar, Europhys. Lett. **87**, 60002 (2009).
[61] Y. Kantor and M. Kardar, Phys. Rev. E **79**, 041109 (2009).
[62] B. Cui, B. Lin, S. Sharma, and S. A. Rice, J. Chem. Phys. **116**, 3119 (2002).
[63] B. Lin, M. Meron, B. Cui, S. A. Rice, and H. Diamant, Phys. Rev. Lett. **94**, 216001 (2005).
[64] A. Huerta, T. Bryk, V. M. Pergamenshchik, and A. Trokhymchuk, Front. Phys. **9**, 636052 (2021).
[65] H. J. Jonas, P. Schall, and P. G. Bolhuis, J. Chem. Phys. **157**, 094903 (2022).
[66] R. Fantoni, Eur. Phys. J. B **96**, 155 (2023).
[67] L. Tonks, Phys. Rev. **50**, 955 (1936).
[68] J. M. Yeomans, *Statistical Mechanics of Phase Transitions* (Clarendon Press, Oxford, UK, 1992).
[69] See Supplemental Material at http://link.aps.org/supplemental/10.1103/PhysRevE.110.014702 for additional information on the analytical solution of the eigenvalue problem for the M1 system.
[70] This calculation is done using the method of Ref. [13].